PROCEEDINGS OF SCIENCE

# Measurement of the ratio of branching fractions $\mathscr{B}(B^0 \to D^{*-}\tau^+\nu_\tau)/\mathscr{B}(B^0 \to D^{*-}\mu^+\nu_\mu)$ with hadronic $\tau$ three-prong decays

**Guy Wormser***
*on behalf of BABAR and LHCb collaborations*
*LAL Orsay, France*
*E-mail:* wormser@lal.in2p3.fr

A measurement of the ratio of semileptonic branching fractions $\mathscr{R}(D^{*-}) \equiv \mathscr{B}(B^0 \to D^{*-}\tau^+\nu_\tau)/\mathscr{B}(B^0 \to D^{*-}\mu^+\nu_\mu)$ is performed using a data sample of proton-proton collisions, corresponding to an integrated luminosity of $3\,\text{fb}^{-1}$, collected by the LHCb experiment at center-of-mass energies of 7 and 8 TeV. For the first time $\mathscr{R}(D^{*-})$ is determined using the $\tau$ lepton decay with three charged pions in the final state. The $B^0 \to D^{*-}\tau^+\nu_\tau$ yield is normalized to that of the $B^0 \to D^{*-}\pi^+\pi^-\pi^+$ mode. A measurement of $\mathscr{B}(B^0 \to D^{*-}\tau^+\nu_\tau)/\mathscr{B}(B^0 \to D^{*-}\pi^+\pi^-\pi^+) = 1.93 \pm 0.13 \pm 0.17$ is obtained, where the first uncertainty is statistical and the second systematic. The value of $\mathscr{B}(B^0 \to D^{*-}\tau^+\nu_\tau) = (1.39 \pm 0.09 \pm 0.12 \pm 0.06)\%$ is obtained, where the third uncertainty is due to the limited knowledge of the branching fraction of the normalization mode. Using the well-measured branching fraction of the $B^0 \to D^{*-}\mu^+\nu_\mu$ decay, a value of $\mathscr{R}(D^{*-}) = 0.285 \pm 0.019 \pm 0.025 \pm 0.013$ is established, where the first uncertainty is statistical, the second systematic, and the third is due to the limited knowledge of the branching fractions of the normalization and of the $B^0 \to D^{*-}\mu^+\nu_\mu$ modes. This measurement is in agreement with the Standard Model prediction and with previous results. The present systematic uncertainty can be reduced by joint efforts of the LHCb, BABAR, BELLE and BES collaborations. This novel analysis technique will also enable the search for SM deviations in the event distributions, in addition to the event yield, thanks to its unique capability to select high statistics ( a few thousands events) highly enriched ( 50%) in semitauonic decays. LHCb will also use the exact same method to perform the measurement of all other B hadrons semitauonic decays, including those coming from $\Lambda_b^0$ and $B_c^+$ hadrons.

*The 15th International Conference on Flavor Physics & CP Violation*
*5-9 June 2017*
*Prague, Czech Republic*

*Speaker.





PoS(FPCP2017)006

## 1. Introduction

In the Standard Model (SM), the electroweak couplings are independent of the lepton family. This lepton universality can be violated in many models that extend the SM by adding interactions with stronger couplings to the third generation. Being mediated by a single $W$ boson, semileptonic decays of $b$-hadrons are a sensitive probe of SM extensions with mass-dependent couplings, *e.g.* models with an enlarged Higgs sector or leptoquarks. In particular, the ratios of branching fractions of semi-tauonic decays of $B$ mesons relative to decays involving lighter lepton families, $\mathscr{R}(D^{(*)}) \equiv \mathscr{B}(B \to D^{(*)}\tau^+\nu_\tau)/\mathscr{B}(B \to D^{(*)}\mu^+\nu_\mu)$, are computed in the SM with a precision at the percent level [1, 2], due to the cancellation of the dominant uncertainties from hadronic effects. The experimental determination of such ratios is also clean, due to the cancellation of many systematic uncertainties.

Measurements of $\mathscr{R}(D)$ and $\mathscr{R}(D^*)$ have been reported by the Babar [3], Belle [4, 5] and LHCb experiments [6], that are consistently higher and average at about $4\sigma$ above the SM predictions[7]. In these measurements, the $\tau$ lepton was always reconstructed in its leptonic decay to electron or muon. A first simultaneous measurement of $\mathscr{R}(D^*)$ and the $\tau$ polarization using the hadronic 1-prong decay was recently released by Belle [8].

This proceeding reports the sensitivity of the first measurement of $\mathscr{R}(D^{*+})$ where the $\tau$ lepton decays into three charged particles (3-prong) in the final state, by using a data sample of proton-proton collisions, corresponding to $3.0 fb^{-1}$ integrated luminosity, collected by the LHCb detector at center-of-mass energies $\sqrt{s} = 7$ and 8 TeV during the LHC Run 1 in 2011-2012. The $D^{*+}$ meson is reconstructed through the $D^{*-} \to \bar{D}^0(\to K^+\pi^-)\pi^-$ decay chain. The final state consists of a $D^*$ meson and 3 pions (plus X). In order to minimize the experimental systematic uncertainties, the $B^0 \to D^{*-}\pi^+\pi^-\pi^+$ decay is chosen as normalization channel, thus leading to a measurement of $\mathscr{R}_{had}(D^*) \equiv \mathscr{B}(B^0 \to D^{*-}\tau^+\nu_\tau)\mathscr{B}(\tau^+ \to 3\pi\nu_\tau)/\mathscr{B}(B^0 \to D^{*-}3\pi)$ that gives a measurement of $\mathscr{R}(D^*)$ by taking the branching fraction of the normalization channel and the well-measured semileptonic decay of the $B^0$ meson in lighter leptons as external inputs. The major background due to $B^0 \to D^*3\pi(X)$ decays (100 times larger than the signal) can be rejected by three orders of magnitude by requiring a decay topology where the $\tau$ decay vertex lies downstream of the $B^0$ decay vertex. This technique is not effective on physics backgrounds due to $B$ decays into double charm events, the largest one being due to $B \to D^* D_s^+(X)$, since the $3\pi$ vertex is transported away from the $B$ vertex in a similar way as for the signal. Observables based on the kinematics, dynamics and topological structure of these backgrounds are used to suppress them. A multidimensional fit,

where template distributions determined from simulation, corrected by using data control samples when needed, provides the statistical separation of signal from the residual background.

## 2. The LHCb detector

The LHCb detector [9, 10] is a single-arm forward spectrometer covering the pseudorapidity range $2 < \eta < 5$, designed for the study of particles containing b or c quarks.

The online event selection is performed by a trigger [11], which consists of a hardware stage, based on information from the calorimeter and muon systems, followed by a software stage, which applies a full event reconstruction. At the hardware trigger stage, events are selected because either particles other than those in the $D^*$ $3\pi$ system pass any trigger requirements, or the $D^*$ decay products satisfy the hadron trigger requirement. The software trigger is topologically based and requires a two-, three- or four-track secondary vertex with a significant displacement from the primary $pp$ interaction vertices (PV). A multivariate algorithm [12] is used for the identification of secondary vertices consistent with the decay of a $b$ hadron. In addition, at least one of the following conditions must be met: the $D^*$ $3\pi$ system must pass the topological trigger defined above, or the $D^0$ and its decay products must satisfy selection criteria based on particle momenta and transverse momenta, $D^0$ momentum pointing to a PV, and $D^0$ reconstructed mass.

In the simulation, $pp$ collisions are generated using PYTHIA [13] with a specific LHCb configuration [14]. Decays of hadronic particles are described by EVTGEN [15], in which final-state radiation is generated using PHOTOS [16]. The interaction of the generated particles with the detector, and its response, are implemented using the GEANT4 toolkit [17] as described in Ref. [18]. In the generation of signal decays, form factors are used that are derived from Heavy Quark Effective Theory [19]. The experimental values of the corresponding parameters are taken from [7], except for an unmeasured helicity-suppressed component, that is taken from [20].

## 3. Signal selection

In the offline selection, $D^0$ candidates are built from well identified kaons and pions, with good track quality. The invariant mass of the $D^0$ candidate must be compatible within 20 MeV with its known value. The $D^*$ candidates are obtained from $D^0$ candidates by adding a low-energy pion. The difference between the invariant mass of the $D^*$ and $D^0$ candidates must lie within 2.5 MeV of the known value. Three well identified and well reconstructed pions are used to build $\tau$ candidates. They also must satisfy IP-$\chi^2 > 15$. Both $D^0$ and $\tau$ candidates must have vertices with a good $\chi^2$, their momentum vectors must approximately point to the location of one PV. The impact parameter of the $D^0$ candidate with respect to any PV must be greater than $10\sigma$. The flight distance of the $\tau$ candidate with respect to any PV must be greater than $10\sigma$ in the beam direction, and between 0.2 and 0.5 *mm* in the transverse plane. The $B^0$ candidate is built by performing a least-square fit of its decay chain [21]. A requirement for the $\tau$ vertex to be downstream the $B^0$ vertex by at least $4\sigma$ significance, as shown in Fig. 1, rejects the background due to $B \to D^* 3\pi X$ decays by three orders of magnitude. After this requirement, the dominant physical background are double charmed events, the only ones to possess the signal vertex topology, as shown in Fig. 2. A similar

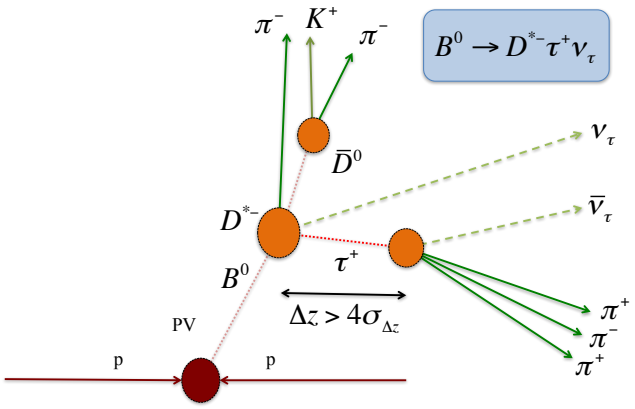


**Figure 1:** Topology of the signal decay. A requirement on the distance between the $3\pi$ and the $B^0$ vertices along the beam direction to be greater than four times its uncertainty is also shown.

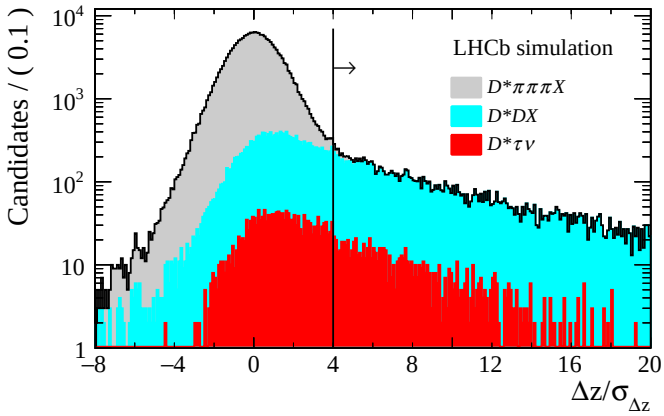


**Figure 2:** Distribution of the distance between the $B^0$ vertex and the $3\pi$ vertex along the z axis, divided by its uncertainty, obtained using simulation. The grey area corresponds to the prompt background component, the blue and red areas to double-charm and signal components, respectively. The vertical line shows the $4\sigma$ requirement used in the analysis to reject the prompt background component.

requirement for the $D^0$ vertex to be downstream the $\tau$ vertex with at least $4\sigma$ significance is used to select the normalization sample.

Physics backgrounds due to partially reconstructed $B$ decays, where at least one additional particle originates from either the $3\pi$, the $B^0$ vertex, or both, are suppressed by requiring a single $B^0$ candidate per event, and by applying an isolation algorithm as follows. If any other charged track in the event, with transverse momentum larger than 250 MeV/$c$ and impact parameter IP with respect to all PVs larger than $2\sigma$, have an IP with respect to either the $B^0$ or $\tau$ vertex smaller than $5\sigma$, the event is rejected. This criterium rejects backgrounds due to $B$ decays with a $D^*D^0$ in the final state by 95% and is still 80% efficient on signal.

Another isolation algorithm, used in the following, computes the multiplicity of reconstructed

tracks, neutral objects and the sum of neutral energy contained in cones of different sizes around the direction of the $\tau$ candidates.

The reconstruction of the kinematics of the signal decay is crucial for signal and background discrimination. Even in the presence of an unreconstructed neutrino, the measurable flight length of the $\tau$ allows to determine its momentum with a 2-fold ambiguity

$$|\vec{p}_\tau| = \frac{(m_{3\pi}^2 + m_\tau^2)|\vec{p}_{3\pi}|\cos\theta \pm E_{3\pi}\sqrt{(m_\tau^2 - m_{3\pi}^2)^2 - 4m_\tau^2|\vec{p}_{3\pi}|^2\sin^2\theta}}{2(E_{3\pi}^2 - |\vec{p}_{3\pi}|^2\cos^2\theta)}, \tag{3.1}$$

where $\theta$ is the angle between the 3 charged pions and the $\tau$ direction; $m_{3\pi}$, $|\vec{p}_{3\pi}|$ and $E_{3\pi}$ are the invariant mass, 3-momentum and energy of the $3\pi$ system, respectively; and $m_\tau$ is the $\tau$ mass. To avoid this ambiguity, the kinematic point where the argument of the root square vanishes can be used. This corresponds to the angle:

$$\theta_{max} = \arcsin\left(\frac{m_\tau^2 - m_{3\pi}^2}{2m_\tau|\vec{p}_{3\pi}|}\right). \tag{3.2}$$

This angle is used to estimate the $\tau$ momentum $|\vec{p}_\tau| = |\vec{p}_\tau(\theta_{max})|$. A similar argument is used to infer the $B^0$ momentum, thereby allowing to reconstruct rest frame variables, such as the $\tau$ decay time and the squared four-momentum transfer of the $B$ to the lepton system $q^2 = (p_B - p_{D^*})^2$ with $p_B$ and $p_{D^*}$ being the four momenta of the $B$ and $D^*$ mesons, with no biases and resolutions sufficient enough to preserve a good discrimination between signal and backgrounds. A partial reconstruction is performed also in the background hypothesis where $B \to D^* D_s^+ (\to 3\pi N)$, $N$ being a massive neutral system, by solving the equation for momentum conservation in two possible ways by applying vectorial algebra.

The Dalitz structure of the $3\pi$ system is a powerful discriminant against backgrounds due to $B$ decays in a $D^*$ and another charm hadron in the final state, especially the $D_s^+$ meson. The three-prong decays of the $\tau$ lepton are dominated by the $a_1$ resonance, therefore the Dalitz plane will exhibit two $\rho$ bands. The $D_s$ decays with $3\pi$ in the final state, instead, are dominated by the $\eta$ and $\eta'$ resonances to a large extent, leading to an enhancement of the Dalitz structure at lower masses.

The suppression of double-charm backgrounds is achieved by combining observables related to the cone-based isolation algorithm (5 variables), to the partial reconstruction in the signal (2 variables) and background (6 variables) hypotheses, to the Dalitz structure of the $3\pi$ system (2 variables), and to the $B^0$ decay kinematics (3 variables), in a multivariate analysis (MVA) method using a boosted decision tree (BDT) [22, 23]. The BDT is trained using signal and background simulations. The background rejection is validated by using three data control samples: a $B \to D^* D_s^+ X$ sample obtained by using the partial reconstruction technique in the background hypothesis; a $B \to D^* D^0 X$ sample obtained by removing the charged particle isolation criterium and requiring a charged kaon around the $3\pi$ vertex with a mass of the K$3\pi$ system compatible with a $D^0$ meson; a $B \to D^* D^+$ sample obtaining requiring positive kaon identification for the pion candidate with charge opposite to that of the other two and a mass of the K$\pi\pi$ system compatible with a $D^+$ meson. A good agreement in the distribution of the input variables to the BDT is observed in data and simulation for all three control samples. The yield for the normalization mode is determined by fitting the invariant mass distribution of the $D^*$ $3\pi$ system around the $B^0$ peak in the normalization

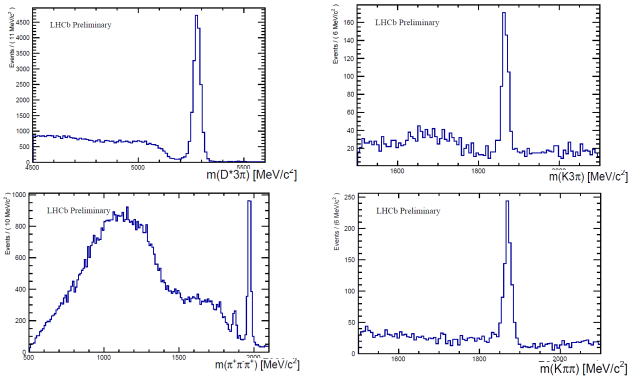


**Figure 3:** Invariant mass distributions : (Top left) $D^*$ $3\pi$ in normal topology (Bottom right) 3pion in detached topology, (Top right) K$3\pi$ in detached topology when an extra charged kaon has been identified as compatible with the $3\pi$ vertex (Bottom Right) $K^-\pi^+\pi^-$ in detached topology where the particle with charge opposite to the two others' has been identified as a good Kaon candidate

sample. Fig.3 exhibits this mass peak, as well as the 3 others which are used to control the backgrounds induced by the $D_s^+$,$D^0$ and $D^+$ mesons. The fitting function is the sum of a Crystal Ball and Gaussian functions for signal, an exponential function for the combinatorial background. A total $17657 \pm 164_{stat} \pm 64_{syst} \pm 22_{D_s sub}$ candidates are found, where the first uncertainty is statistical, the second systematic and the third refers to the subtraction of a small contribution of $151 \pm 22$ candidates due to $B \to D^* D_s^+ (\to 3\pi)$ decays.

## 4. The $D_s^+$ decay model

At low BDT values, the data sample consists about 85% of $D^* D_s^+$ events and is used to refine the $D_s^+$ decay model used in the MC simulation. A simultaneous fit of 4 mass spectra (min mass($\pi^+\pi^-$), max mass ($\pi^+\pi^-$), mass($\pi^+\pi^+$) , mass ($3\pi$) allows to fix the relatives proportions of the four main categories of $D_s^+$ decays into 3pions : $\eta\pi$ +X, $\eta'\pi$ +X, $\phi, \omega$+X, R$\pi^+\pi^-\pi^+$. The distribution (min mass($\pi^+\pi^-$) is playing a specially useful role because it constrains the $\eta'$ component through the low mass enhancement specific to the $\eta' \to \eta\pi^+\pi^-$, and therefore constrains the rate of only signal-like decay channel of the $D_s^+$ meson, $D_s^+ \to \eta'\pi$ +X with $\eta' \to \rho\gamma$. Fig.4 shows the minimum mass($\pi^+\pi^-$) with the four $D_s^+$ components mentionned above and the very good agreement obtained in that fit. The relative contribution of each mode in the high BDT output region used for the signal fit are inferred using simulation. The signal yield is obtained by a three-dimensional fit to the data, in a region above the threshold previously mentioned in the BDT output, by using templates obtained on simulation. The fit variables are: the $\tau$ decay time, the squared invariant mass of the lepton pair $q^2$, and the output of the BDT. The control samples defined above are also used to check that the simulation well reproduces the expected distributions on data, and to correct the simulation otherwise.

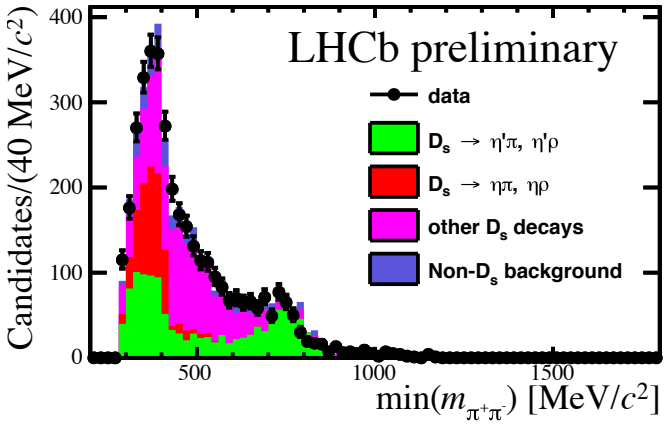


**Figure 4:** Fit to the $min(m_{\pi^+\pi^-})$ distribution in a sample enriched in $D^*D_s$ decays, obtained by requiring the BDT output below a threshold. The different fit components correspond to $D_s$ decays with $\eta$ (red), $\eta'$ (green), all the rest (magenta) in the final state, and non-$D_s$ decays (grey). The total fit model is the solid histogram, points correspond to data.

## 5. Templates determination and signal extraction

The signal template is the sum of two terms, due to $\tau \to 3\pi$ and $\tau \to 3\pi\pi^0$ decay, where the yield for the latter scaled with the former through a proportionality factor determined by their relative branching fractions and selection efficiencies. A contribution due to $B \to D^{**}\tau\nu_\tau$ decays, with the $D^*$ being produced in the $D^{**}$ decay chain, is also linked to the signal yield through a proportionality factor determined from simulation, and validated on a sample where the narrow $D_1^0(2420)$ and $D_2^{*0}(2460)$ resonances are reconstructed in their $D^*\pi$ decay.

The background due to $H_b \to D^*D_s^+X$ decays, $H_b$ being a generic $b$ hadron, is divided into contributions from $B^0 \to D^{*-}D_s^+$, $B^0 \to D^{*-}D_s^{*-}$, $B^0 \to D^{*-}D_{s0}^{*+}$, $B^0 \to D^{*-}D_{s1}^{\prime+}$, $B^{0,+} \to D^{**}D_s^+X$, $B_s^0 \to D^{*-}D_s^+X$. Their relative contributions are constrained by using the results of a fit, to the $D^*$ $3\pi$ invariant mass on a data control sample consisting of these decays, where the $D_s^+$ meson is reconstructed through its exclusive decay in $3\pi$. The relative amount of each contribution obtained from this fit is used to rescale the simulation when preparing the templates to be used in the final fit.

The number of floating parameters in the fit is 11. The $B \to D^*D^0X$ background is subdivided in two contributions, according to whether the $3\pi$ originate from the same $D^0$ vertex, or where at least one pion originate from the $D^0$ vertex and the other two from elsewhere. The contribution of the former is constrained, based on the yield obtained on the $D^0 \to K3\pi$ control sample where a kaon compatible with the $3\pi$ vertex is found. The template shape is also taken from the same control sample. The yield of the latter is a free parameter in the fit. The yield of the $B \to D^*D^+X$ background is a free parameter. The template shape is taken from the corresponding control sample. A residual contribution of $B \to D^*3\pi X$ decays is included, its contribution constrained by means of the $B^0 \to D^*3\pi$ exclusive peak.

The combinatorial background is divided in two contributions, depending on whether the $D^*$

meson is real or fake. In the first case, the $D^*$ and the $3\pi$ originate from different $B$ decays. The shape is taken from simulation. A sample of candidates where the $D^*$ and the $3\pi$ system have the same charge is used to normalize data and simulation above the $B$ meson mass. The fake $D^*$ background is parameterized and constrained by using the events in the $D^0$ sidebands.

Uncertainties in the template shape, that originate from the finite size of the simulation sample, are taken into account in the fit likelihood by using the Beeston-Barlow procedure [24].

By taking into account the ratio of efficiencies between signal and normalization $\varepsilon_{sig}/\varepsilon_{norm}$, correction factors due to PID and trigger mismodelling between data and MC, the sum of the branching fractions for the $\tau \to 3\pi$ and $\tau \to 3\pi\pi^0$ decays, properly reweighted to take into account efficiency differences, the value for the $B^0 \to D^*3\pi$ and $B^0 \to D^{*-}\mu\nu_\mu$, R(D*) can be determined. We obtain a statistical error of 6.7% for the Run1 data sample. This is the smallest statistical reported so far for a single measurement of R(D*). The results of the fit are shown in Fig. 5. The

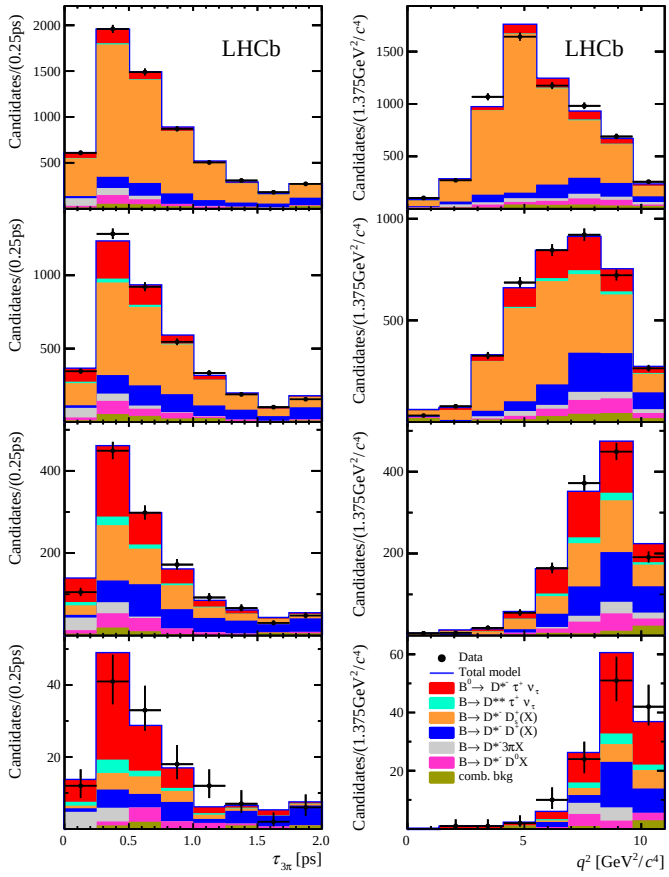


**Figure 5:** Distributions of (left) the $3\pi$ decay time, $\tau_{3\pi}$, and (right) $q^2$ in four different BDT bins. The BDT output and the signal purity increase from top to bottom. The various fit components are described in the legend.

signal yield is corrected for a small bias of 40 candidates, due to the finite size of the templates

**Table 1:** Relative systematic uncertainties on $\mathscr{R}(D^{*-})$.

| Source | $\delta R(D^{*-})/R(D^{*-})[\%]$ |
|---|---|
| Simulated sample size | 4.7 |
| Empty bins in templates | 1.3 |
| Signal decay model | 1.8 |
| $D^{**}\tau\nu$ and $D_s^{**}\tau\nu$ feeddowns | 2.7 |
| $D_s^+ \to 3\pi X$ decay model | 2.5 |
| $B \to D^{*-}D_s^+X$, $B \to D^{*-}D^+X$, $B \to D^{*-}D^0X$ backgrounds | 3.9 |
| Combinatorial background | 0.7 |
| $B \to D^{*-}3\pi X$ background | 2.8 |
| Efficiency ratio | 3.9 |
| Total uncertainty | 8.9 |

from simulation, as detailed below, giving $N_{sig} = 1273 \pm 85$ candidates. A measurement of

$$\mathscr{K}(D^{*-}) = 1.93 \pm 0.13\,(\text{stat}) \pm 0.17\,(\text{syst}) \tag{5.1}$$

is obtained by multiplying the ratio of the yields for signal and normalization modes by the ratio of the two respective efficiencies. A correction factor $1.056 \pm 0.025$ is applied when computing $\mathscr{K}(D^*)$ in order to account for discrepancies between data and simulation, and for a small feed-down contribution from $B_s^0 \to D_s^{**-}\tau^+\nu_\tau$ decays, where $D_s^{**-} \to D^{*-}K^0$.

A value of $\mathscr{B}(B^0 \to D^{*-}\tau^+\nu_\tau) = (1.39 \pm 0.09\,(\text{stat}) \pm 0.12\,(\text{syst}) \pm 0.06) \times 10^{-2}$ is obtained by using $\mathscr{B}(B^0 \to D^{*-}3\pi) = (7.21 \pm 0.29) \times 10^{-3}$ from Ref. [25]. A determination of $\mathscr{R}(D^{*-}) = 0.285 \pm 0.019\,(\text{stat}) \pm 0.025\,(\text{syst}) \pm 0.013$ is obtained by using $\mathscr{B}(B^0 \to D^{*-}\mu^+\nu_\mu) = (4.88 \pm 0.10) \times 10^{-2}$ from Ref. [26]. In both results, the third uncertainty is due to the limited knowledge of the external branching fraction(s).

## 6. Systematic uncertainties

Systematic uncertainties on $\mathscr{R}(D^{*-})$ are reported in Table 1. The uncertainty due to the limited size of the simulated samples is computed by repeatedly sampling each template with a bootstrap procedure, performing the fit, and taking the standard deviation of the results obtained. The limited size of the simulated samples also contributes to the systematic uncertainty on the efficiencies for signal and normalization modes. The existence of empty bins in the templates used in the fit, due to the limited size of the simulated samples, introduces a positive bias of 3% in the determination of the signal yield. This corresponds to a correction of 40 candidates, with an uncertainty of 1.3%.

The systematic uncertainty associated to the signal decay model derives from the limited knowledge of the form factors and the $\tau$ polarization, from possible contributions from other $\tau$ decay modes, and from the relative branching fractions and selection efficiencies of $\tau^+ \to 3\pi\pi^0\overline{\nu}_\tau$ and $\tau^+ \to 3\pi\overline{\nu}_\tau$ decays. Uncertainties due to the knowledge of the $D^{**}\tau^+\nu_\tau$ contribution to the signal yield are estimated using a control sample where one additional charged pion originating from the $B$ vertex is identified. The observed yield of the narrow $D_1(2420)^0$ resonance is used to

infer a 40% uncertainty on the yield of $D^{**}\tau^+\nu_\tau$ decays relative to that of the signal. A systematic uncertainty is also assigned to take into account the feeddown from $B_s^0$ decays into $D_s^{**-}\tau^+\nu_\tau$.

The uncertainty due to the knowledge of the $D_s^+$ decay model is estimated by repeatedly varying the correction factors of the templates within their uncertainties, as determined from the associated control sample, and performing the fit. The spread of the fit results is assigned as the corresponding systematic uncertainty. The template shapes of the $D^{*-}D_s^+$, $D^{*-}D^0$ and $D^{*-}D^+$ backgrounds depend on the dynamics of the corresponding decays. Empirical variations of the kinematic distribution are performed, and the spread of the fit results is taken as a systematic uncertainty. A similar procedure is applied to the template for the combinatorial background. Other sources of systematic uncertainty arise from the inaccuracy on the yields of the various background contributions, and from the limited knowledge of the normalization and the resonant structure of the residual background due to $B^0 \to D^{*-}3\pi X$ decays.

Systematic effects on the efficiencies for signal and normalization partially cancel in the ratio. The trigger efficiency depends on the distributions of the decay time of the $3\pi$ system and the invariant mass of the $D^{*-}$ $3\pi$ system. These distributions differ between the signal and normalization modes, and the difference of the trigger efficiency for these two decays is taken into account.

## 7. Results

The first measurement of $\mathscr{R}(D^{*-})$ with three-prong $\tau$ decays has been performed by using a technique that is complementary to all previous measurements of this quantity and offers the possibility to study other $b$-hadron decay modes in a similar way. The result, $\mathscr{R}(D^*) = 0.285 \pm 0.019\,(\text{stat}) \pm 0.025\,(\text{syst}) \pm 0.013\,(\text{ext})$, is one of the most precise single measurements performed so far. It is one standard deviation higher the than the SM calculation $(0.252 \pm 0.003)$ of Ref. [1], and consistent with previous determinations. An average of this measurement with the LHCb result using $\tau^+ \to \mu^+\nu_\mu\overline{\nu}_\tau$ decays [27], accounting for small correlations due to form factors, $\tau$ polarization and $D^{**}\tau^+\nu_\tau$ feeddown, gives $\mathscr{R}(D^{*-}) = 0.306 \pm 0.016\,(\text{stat}) \pm 0.022\,(\text{syst})$, consistent with the world average and 2.1 standard deviations above the SM prediction. A summary of all R(D*) measurements up to now is presented on Fig. 6. The latest update from HFLAV [26] including this result( Fig. 7) indicates that, although this result moves the WA R(D*) slightky closer to its SM expected value, nevertheless, due to its small uncertainties, the new combined disagreement between R(D) and R(D*) grows from 4.0 to $4.1\sigma$.

## 8. Prospects

LHCb Run2 data sample contains about 3 times more $D^*$ events per $\text{fb}^{-1}$ because of the higher $b\bar{b}$ cross section at 13 TeV and more efficient trigger conditions. The data sample using data already on tape today, can therefore be tripled and reach a statistical precision significantly better than the present world average. More over, LHCb can and will study using the $\tau$ muonic and hadronic channels all the other semitauonic decays, namely $B_s^0$ to $D_s^+\tau\nu$, $\Lambda_b^0$ to $\Lambda_c^+\tau\nu B_c^+$ to $J/\psi\,\tau\nu$, $B^0$ and $B^+$ to $D^0\tau\nu$ and $D^+\tau\nu$. The relative precision of the R measurement in all these channels will depend of the specific combination of production yield, reconstructible final states' branching fractions, trigger conditions and background levels, but one could estimate that they can end up to

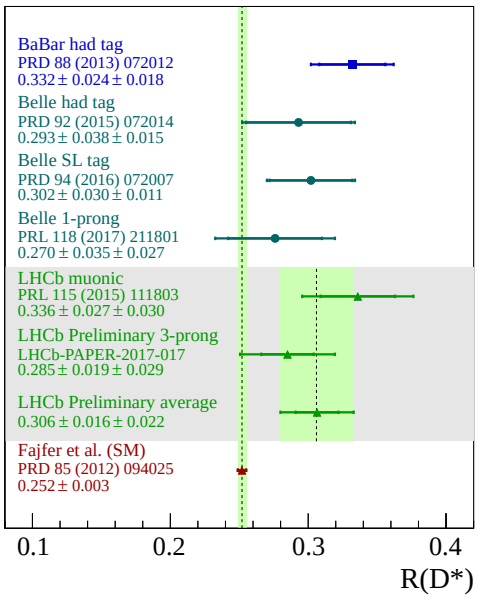


**Figure 6:** Results of this analysis together with all R(D*) measurements reported so far, together with the new R(D*) LHCb average determination, compared to the SM prediction

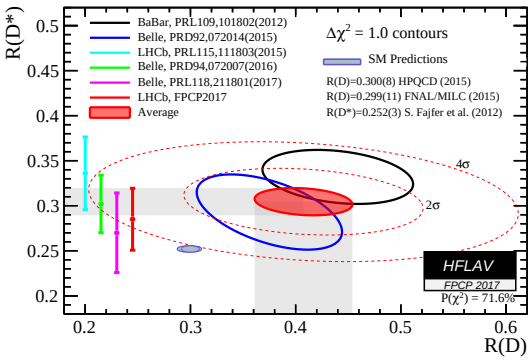


**Figure 7:** R(D) and R(D*) measurements reported so far including this result, with the HFLAV [26] determination of the World average (WA), and compared to the SM prediction

be rather similar at the 10% level. The diversity of all these channels, as well as the different values of the spin of spectator particle (0 for $D_s^+$,$D^0$ and $D^+$, 1 for $D^*$ and $J/\psi$ and 1/2 for $\Lambda_c^+$) will offer an uncomparable probe of deviations from SM due to Lepton Universality Violation. It has also be stressed that the $3\pi$ hadronic $\tau$ analysis channel will offer, in all these cases, the possibility to study potential deviations from SM prediction beyond the mere event yield, by a study of relevant angular and kinematic distributions thanks to the large purity (typically 50%) and high statistics (typically 1000 events) that can be uniquely reached with the novel method described in this proceedings.

## Acknowledgments

We express our gratitude to our colleagues in the CERN accelerator departments for the excellent performance of the LHC. We thank the technical and administrative staff at the LHCb institutes. We acknowledge support from CERN and from the national agencies: CAPES, CNPq, FAPERJ and FINEP (Brazil); MOST and NSFC (China); CNRS/IN2P3 (France); BMBF, DFG and MPG (Germany); INFN (Italy); NWO (The Netherlands); MNiSW and NCN (Poland); MEN/IFA (Romania); MinES and FASO (Russia); MinECo (Spain); SNSF and SER (Switzerland); NASU (Ukraine); STFC (United Kingdom); NSF (USA). We acknowledge the computing resources that are provided by CERN, IN2P3 (France), KIT and DESY (Germany), INFN (Italy), SURF (The Netherlands), PIC (Spain), GridPP (United Kingdom), RRCKI and Yandex LLC (Russia), CSCS (Switzerland), IFIN-HH (Romania), CBPF (Brazil), PL-GRID (Poland) and OSC (USA). We are indebted to the communities behind the multiple open source software packages on which we depend. Individual groups or members have received support from AvH Foundation (Germany), EPLANET, Marie Skłodowska-Curie Actions and ERC (European Union), Conseil Général de Haute-Savoie, Labex ENIGMASS and OCEVU, Région Auvergne (France), RFBR and Yandex LLC (Russia), GVA, XuntaGal and GENCAT (Spain), Herchel Smith Fund, The Royal Society, Royal Commission for the Exhibition of 1851 and the Leverhulme Trust (United Kingdom).

## References

## References

[1] S. Fajfer, J. F. Kamenik, and I. Nisandzic, *On the $B \to D^*\tau\overline{\nu}_\tau$ sensitivity to new physics*, Phys. Rev. **D85** (2012) 094025, arXiv:1203.2654.

[2] D. Bigi and P. Gambino, *Revisiting $B \to D\ell\nu$*, Phys. Rev. **D94** (2016) 094008, arXiv:1606.08030.

[3] BaBar collaboration, J. P. Lees *et al.*, *Evidence for an excess of $\bar{B} \to D^*\tau^-\overline{\nu}_\tau$ decays*, Phys. Rev. Lett. **109** (2012) 101802, arXiv:1205.5442.

[4] Belle collaboration, M. Huschle *et al.*, *Measurement of the branching ratio of $\bar{B} \to D^{(*)}\tau^-\overline{\nu}_\tau$ relative to $\bar{B} \to D^{(*)}\ell^-\overline{\nu}_\ell$ decays with hadronic tagging at Belle*, Phys. Rev. **D92** (2015) 072014, arXiv:1507.03233.

[5] Belle collaboration, Y. Sato *et al.*, *Measurement of the branching ratio of $\bar{B}^0 \to D^{*+}\tau^-\overline{\nu}_\tau$ relative to $\bar{B}^0 \to D^{*+}\ell^-\overline{\nu}_\ell$ decays with a semileptonic tagging method*, Phys. Rev. **D94** (2016) 072007, arXiv:1607.07923.

[6] LHCb collaboration, R. Aaij *et al.*, *Measurement of the ratio of branching fractions $\mathscr{B}(\bar{B}^0 \to D^{*+}\tau^-\overline{\nu}_\tau)/\mathscr{B}(\bar{B}^0 \to D^{*+}\mu^-\overline{\nu}_\mu)$*, Phys. Rev. Lett. **115** (2015) 111803, arXiv:1506.08614.

[7] Y. Amhis *et al.*, *Averages of b-hadron, c-hadron, and $\tau$-lepton properties as of summer 2016*, arXiv:1612.07233.

[8] Belle collaboration, S. Hirose *et al.*, *Measurement of the $\tau$ lepton polarization and $R(D^*)$ in the decay $\bar{B} \to D^*\tau^-\overline{\nu}_\tau$*, Phys. Rev. Lett. **118** (2017) 211801, arXiv:1612.00529.

[9] LHCb collaboration, A. A. Alves Jr. *et al.*, *The LHCb detector at the LHC*, JINST **3** (2008) S08005.

[10] LHCb collaboration, R. Aaij *et al.*, *LHCb detector performance*, Int. J. Mod. Phys. **A30** (2015) 1530022, arXiv:1412.6352.

[11] R. Aaij *et al.*, *The LHCb trigger and its performance in 2011*, JINST **8** (2013) P04022, arXiv:1211.3055.

[12] V. V. Gligorov and M. Williams, *Efficient, reliable and fast high-level triggering using a bonsai boosted decision tree*, JINST **8** (2013) P02013, arXiv:1210.6861.

[13] T. Sjöstrand, S. Mrenna, and P. Skands, *PYTHIA 6.4 physics and manual*, JHEP **05** (2006) 026, arXiv:hep-ph/0603175; T. Sjöstrand, S. Mrenna, and P. Skands, *A brief introduction to PYTHIA 8.1*, Comput. Phys. Commun. **178** (2008) 852, arXiv:0710.3820.

[14] I. Belyaev *et al.*, *Handling of the generation of primary events in Gauss, the LHCb simulation framework*, J. Phys. Conf. Ser. **331** (2011) 032047.

[15] D. J. Lange, *The EvtGen particle decay simulation package*, Nucl. Instrum. Meth. **A462** (2001) 152.

[16] P. Golonka and Z. Was, *PHOTOS Monte Carlo: A precision tool for QED corrections in Z and W decays*, Eur. Phys. J. **C45** (2006) 97, arXiv:hep-ph/0506026.

[17] Geant4 collaboration, J. Allison *et al.*, *Geant4 developments and applications*, IEEE Trans. Nucl. Sci. **53** (2006) 270; Geant4 collaboration, S. Agostinelli *et al.*, *Geant4: A simulation toolkit*, Nucl. Instrum. Meth. **A506** (2003) 250.

[18] M. Clemencic *et al.*, *The LHCb simulation application, Gauss: Design, evolution and experience*, J. Phys. Conf. Ser. **331** (2011) 032023.

[19] I. Caprini, L. Lellouch, and M. Neubert, *Dispersive bounds on the shape of $\bar{B} \to D^* \ell \overline{\nu}$ form-factors*, Nucl. Phys. **B530** (1998) 153, arXiv:hep-ph/9712417.

[20] J. G. Korner and G. A. Schuler, *Exclusive semileptonic heavy meson decays including lepton mass effects*, Z. Phys. **C46** (1990) 93.

[21] W. D. Hulsbergen, *Decay chain fitting with a Kalman filter*, Nucl. Instrum. Meth. **A552** (2005) 566, arXiv:physics/0503191.

[22] L. Breiman, J. H. Friedman, R. A. Olshen, and C. J. Stone, *Classification and regression trees*, Wadsworth international group, Belmont, California, USA, 1984.

[23] Y. Freund and R. E. Schapire, *A decision-theoretic generalization of on-line learning and an application to boosting*, J. Comput. Syst. Sci. **55** (1997) 119.

[24] R. Barlow and C. Beeston, *Fitting using finite monte carlo samples*, Computer Physics Communications **77** (1993) 219 .

[25] Particle Data Group, C. Patrignani *et al.*, *Review of particle physics*, Chin. Phys. **C40** (2016) 100001, and 2017 update.

[26] Heavy Flavor Averaging Group, Y. Amhis *et al.*, *Averages of b-hadron, c-hadron, and $\tau$-lepton properties as of summer 2016*, arXiv:1612.07233, updated results and plots available at http://www.slac.stanford.edu/xorg/hfag/.

[27] LHCb collaboration, R. Aaij *et al.*, *Measurement of the ratio of branching fractions $\mathscr{B}(\bar{B}^0 \to D^{*+}\tau^-\overline{\nu}_\tau)/\mathscr{B}(\bar{B}^0 \to D^{*+}\mu^-\overline{\nu}_\mu)$*, Phys. Rev. Lett. **115** (2015) 111803, arXiv:1506.08614.